

AIRCRAFT BRAKING DYNAMICS AND BRAKE SYSTEM MODELING FOR FAULT DETECTION AND ISOLATION

Lucas Cardoso Navarro

ITA

São José dos Campos, São Paulo,
Brazil

Luiz Carlos Sandoval Goes

ITA

São José dos Campos, São Paulo,
Brazil

ABSTRACT

Due to the increasing complexity of aeronautical systems, it became more and more important to detect accurately failures that may occur, avoiding costs with maintenance and time out of operation. With the aid of modeling techniques and computational software, it became possible to analyze systems behaviors under normal and failures conditions, helping to prevent these problems. In this work, an aircraft anti-skid brake system is considered as a study case. Therefore, the aircraft dynamics and the main elements of the hydraulic brake system, such as servo valve, hydraulic line and brake actuator, are modeled and simulated using the software Simulink®. The integration of the hydraulic brake system model with the aircraft braking dynamics is made, being possible to simulate the aircraft anti-skid control system. In the hydraulic brake system model, some common faults are introduced in order to observe its impacts on the aircraft braking performance. A fault detection and isolation (FDI) method based on analytical redundancy relations (ARRs) is proposed. The ARRs are equations relating the system constraints, receiving as inputs the system behavior model parameters, sources and measurements (sensors readings as sources). The numerical evaluation of these equations generates the residuals. The residual value indicates the systems deviation level from its normal operation. The coupling of the Simulink® system behavior model with the ARRs is presented, permitting the residual analyses for each failure mode introduced in the hydraulic brake system model.

Keywords: Aircraft anti-skid brake system, Fault detection and isolation, ARRs, Hydraulic Brake System, Physical Modeling

MODELING METHOD

To perform the system modeling, the physical modeling was used. This methodology is a simplified representation of a system through idealized elements with the intention of representing the dynamics phenomena of real systems. These elements simulate supply sources, as well as the storage, dissipation and transformation of the system energy. Based on this concept, it is possible to represent the system in a unified way, taking into account only the elements energy interactions. Thus, in this work, electrical equivalents were used to perform mathematical modeling, representing the entire system.

Aircraft and wheel dynamics modeling

The main part of the aircraft kinetics energy is dissipated by the brake system during braking time. The brake force is generated from the brake system actuators. The Figure 1 shows the forces acting on the aircraft and wheels during braking time, its electrical equivalent and the state equations extracted from it.

Servo Valve, hydraulic line and brake actuator modeling

The Figure 2 a) shows the servo valve schematic and 2 b), its corresponding electrical equivalent circuit. This valve controls the brake pressure. Analyzing the circuit shown at Figure 2 b), it is possible to extract the state equations that describes the hydraulic brake system dynamics. The Figure 3 relates all the states and parameters used for the modeling.

Anti-skid brake system

The anti-skid system model is based on the differential equations that describe the wheel and aircraft dynamics. The Figure 4 illustrates the anti-skid system control loop diagram. A PI controller modulates the voltage acting on the servo valve, modulating the pressure that drives the brakes in order to maintain the slip ratio at an optimum position, ensuring a maximum efficiency at the brake moment. To perform the simulations, a Simulink model was created. With the model it was possible to simulate the aircraft braking performance for several conditions and it was noticed a great loss in the braking performance with the faults introduction in the servo valve.

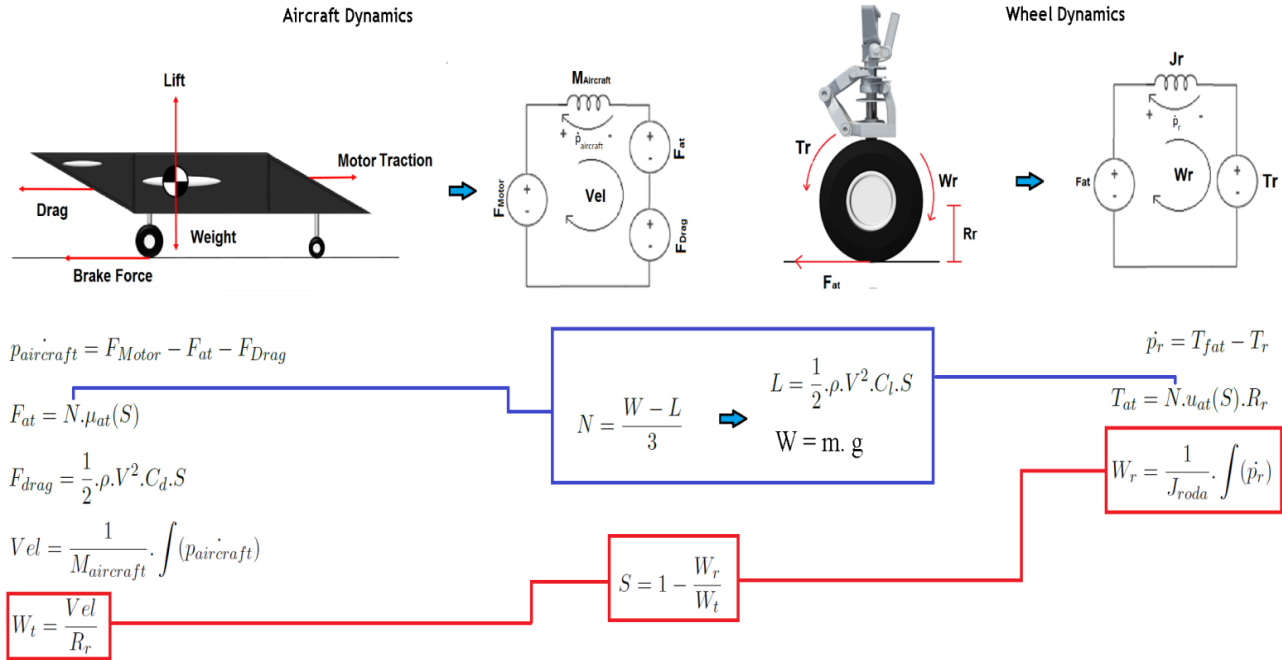


Figure 4 – Aircraft and wheels free body diagram during braking time, the corresponding electrical equivalent and state equations

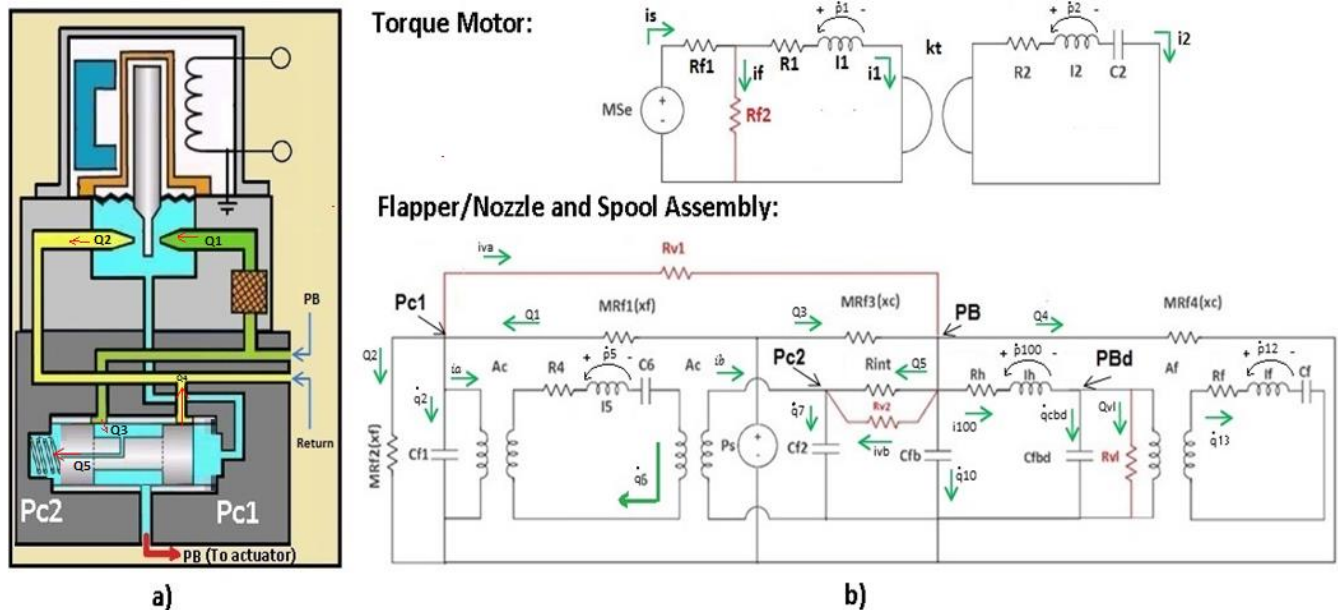


Figure 2 – a) Servo-valve schematic. b) Servo-valve, hydraulic line and brake actuator electrical equivalent

$$\begin{aligned} \dot{p}_1 &= \frac{M_{SE} - R_{f1} \cdot \frac{p_1}{I_1} - (\frac{R_{f1}}{R_{f2}} + 1) \cdot (R_{f1} \cdot \frac{p_1}{I_1} + \frac{p_2}{I_2} \cdot K_t)}{(\frac{R_{f1}}{R_{f2}} + 1)} \\ \dot{p}_2 &= V_2 - R_2 \cdot \frac{p_2}{I_2} - \frac{9C_2}{C_2} \\ \dot{q}_{C2} &= \frac{p_2}{I_2} \\ \dot{q}_2 &= Q_1 - Q_2 - i_{va} - i_b \begin{cases} Q_1 = C_d \cdot \pi \cdot dn \cdot xf \cdot \sqrt{\frac{2}{\rho} \cdot (P_s - P_{c1})} \\ Q_2 = C_d \cdot \pi \cdot dn \cdot (L - xf) \cdot \sqrt{\frac{2}{\rho} \cdot (P_{c1})} \\ i_{va} = \frac{P_{c1} - P_b}{R_{v1}} \\ i_b = Ac \cdot \frac{p_2}{p_1} \end{cases} \\ \dot{p}_5 &= V_1 - V_{R4} - V_{C6} - V_2 \begin{cases} V_1 = Ac \cdot P_{c1} \\ V_{R4} = \frac{p_5}{R_4} \cdot R_4 \\ V_{C6} = \frac{p_5}{C_6} \\ V_2 = Ac \cdot \frac{p_5}{C_7} \end{cases} \\ \dot{q}_{bd} &= i_{100} - Q_{cl} - i_e \begin{cases} i_{100} = Ac \cdot i_f \\ Q_{cl} = C_d \cdot Avl \cdot \sqrt{\frac{2}{\rho} \cdot (PB_d)} \\ i_e = Af \cdot \frac{p_5}{p_1} \end{cases} \\ \dot{p}_{100} &= V_{Cfb} - V_{Rb} - V_{Cfb} \begin{cases} V_{Cfb} = PB \\ V_{Rb} = R_b \cdot \frac{p_{100}}{I_{100}} \\ V_{Cfb} = PBd \end{cases} \\ \dot{q}_7 &= Q_5 + i_b + i_{eb} \begin{cases} Q_5 = \frac{PB - P_{c2}}{R_{int}} \\ i_b = Ac \cdot \frac{p_7}{p_5} \\ i_{eb} = \frac{PB - P_{c2}}{R_{v2}} \end{cases} \\ \dot{q}_{10} &= Q_3 - Q_4 - Q_5 - i_{eb} + i_{va} - i_{100} \begin{cases} Q_3 = C_d \cdot w \cdot xc \cdot \sqrt{\frac{2}{\rho} \cdot (P_s - PB_{bl})} \\ Q_4 = C_d \cdot w \cdot xc \cdot \sqrt{\frac{2}{\rho} \cdot (PB_{bl})} \\ Q_5 = \frac{PB - P_{c2}}{R_{int}} \\ i_{eb} = \frac{PB - P_{c2}}{R_{v2}} \\ i_{va} = \frac{P_{c1} - P_b}{R_{v1}} \\ i_{100} = \frac{p_{100}}{I_{100}} \end{cases} \\ \dot{p}_{12} &= V_f - V_{Rf} - V_{Cf} \begin{cases} V_f = Ac \cdot PBd \\ V_{Rf} = R_f \cdot \frac{p_{12}}{I_{12}} \\ V_{Cf} = \frac{p_{12}}{C_f} \end{cases} \\ \dot{q}_{13} &= \frac{p_{12}}{I_f} \\ \dot{q}_6 &= \frac{p_5}{I_5} \end{aligned}$$

Flow rate pressure nozzle: $Q_1 = C_d \cdot \pi \cdot dn \cdot xf \cdot \sqrt{\frac{2}{\rho} \cdot (P_s - P_{c1})}$
 Flow rate return nozzle: $Q_2 = C_d \cdot \pi \cdot dn \cdot (L - xf) \cdot \sqrt{\frac{2}{\rho} \cdot (P_{c1})}$
 Flow rate pressure spool nozzle: $Q_3 = C_d \cdot w \cdot xc \cdot \sqrt{\frac{2}{\rho} \cdot (P_s - PB_{bl})}$
 Flow rate return spool nozzle: $Q_4 = C_d \cdot w \cdot xc \cdot \sqrt{\frac{2}{\rho} \cdot (PB_{bl})}$
 Flapper volume: $C_{f1} = \frac{V_{flapper}}{\beta}$
 Spool left side volume: $C_{f2} = \frac{V_{feedback}}{\beta}$
 Spool viscosity: $R_4 = b_{spool}$
 Spool mass: $I_5 = M_{spool}$
 Spool rigidity: $C_6 = \frac{1}{K_{spool}}$
 Internal spool and hydraulic line volume: $C_{fb} = \frac{V_{id}}{\rho}$
 Brake actuator volume: $C_{fbd} = \frac{V_{brake}}{\rho}$
 Pressure right spool side: $P_{c1} = \frac{q_2}{C_{f1}}$
 Brake pressure before brake line: $P_{Bd} = \frac{q_{bd}}{C_{bd}}$
 Fluid resistance between internal and left spool side: $R_{int} = \frac{128 \cdot \mu \cdot L_{int}}{\pi \cdot D_{int}^4}$
 Fluid inertia hydraulic line: $I_h = \frac{L_h \cdot \rho}{A_h}$
 Fluid resistance hydraulic line: $R_h = \frac{128 \cdot \mu \cdot L_h}{\pi \cdot D_h^4}$
 Spool wall leakage right/left side: $R_{v1} = R_{v2} = \frac{128 \cdot \mu \cdot L_{sh}}{\pi \cdot D_{vsh}^4}$
 Hydraulic line leakage flow rate: $Q_{cl} = C_d \cdot D_{cl} \cdot \sqrt{\frac{2}{\rho} \cdot (PB)}$
 Brake pressure: $P_B = \frac{q_{10}}{C_{fb}}$
 Pressure left spool side: $P_{c2} = \frac{q_7}{C_{f2}}$

Af = Brake actuator area
 Avl = Hydraulic line leakage
 Cd = Discharge coefficient
 xc = Spool position
 Ac = Spool wall area
 w = Spool nozzle width
 xf = Flapper position
 dn = Flapper nozzle diameter
 L = Distance between nozzles in the flapper

Figure 3 – State equations derived from the electrical equivalent in the Figure 2 b) and parameters used for the hydraulic brake system modeling also shown in the Figure 2 b)

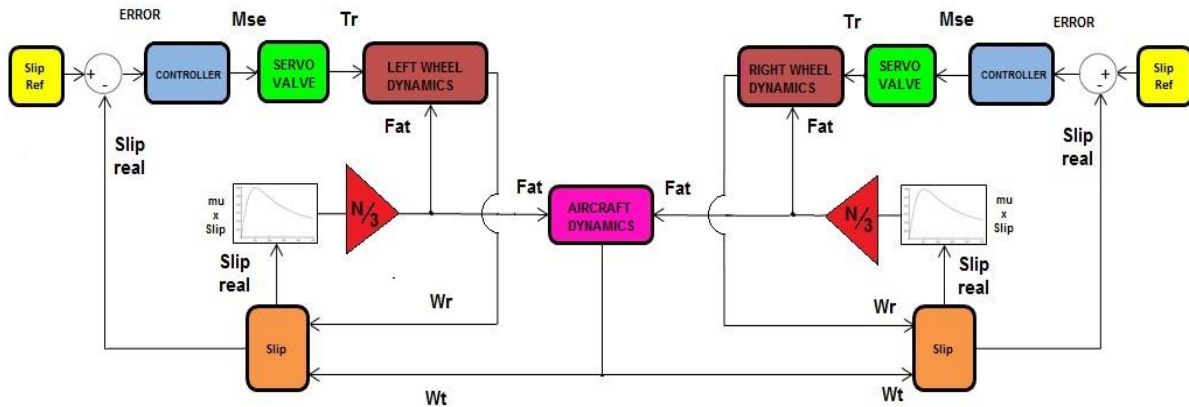


Figure 4 – Anti-skid system control loop diagram

FAULT DETECTION AND ISOLATION METHOD

The first step is to create a behavior model where the state equations describing the dynamic behavior of a given system, can be derived. In this model, some sensors are introduced in order to monitor the states. The second step is to create a diagnostic model. In this model, instead of measuring the states, it will receive from the behavior model the sensor measurement as a source. This way, the equations describing the system dynamics (the system constraints) will be written in terms of the real system sources, original parameters and sensor measurements. Thus, these equations will have a redundancy, creating a real test from the actual system. The Figure 5 shows a mass, damper and spring system, its electrical equivalent behavior model with a flow sensor (mass velocity sensor) and the diagnostic model with the sensor measured source. From the behavior model, the state equation describing the system dynamics is extracted. From the diagnostic model, the ARR equation is extracted. The numerical evaluation of the ARR equation is the residual value. If the sensor measurement comes from the original system, without faults, the residual value (r) must be zero. However, if the sensor measurement comes from the same system, but with some parameter differing from its original value due to some fault, the residual value will differs from zero, indicating the fault. The FDI method was applied, using the servo-valve model. The Figure 6 shows the behavior model with the sensor placement, the diagnostic model and the ARRs extracted from it. With this sensor placement configuration, it is possible to extract the ARRs. Thus, from each measured source, there will be an ARR. The Simulink model linking the behavior model and the diagnostic model, generating the

states and the residuals was developed. The simulations were made introducing some failure modes in the behavior system, making it possible to observe the residual response.

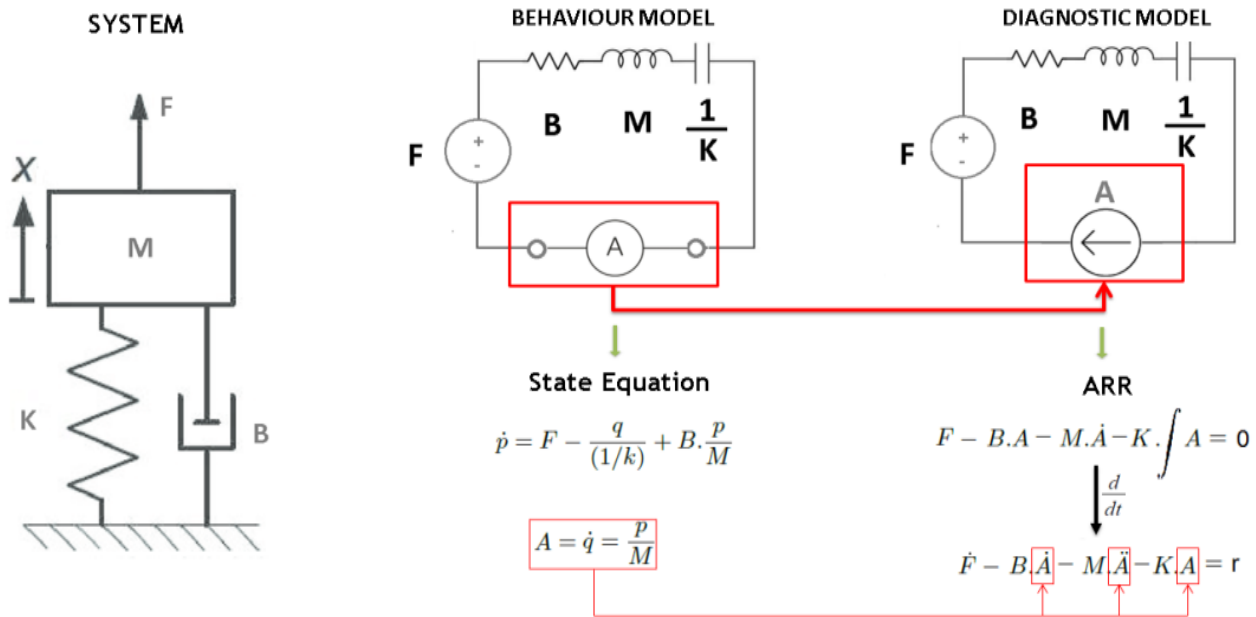


Figure 5 – Mass, spring and dumper system example, electrical equivalent behavior and diagnostic model, state and ARR equations.

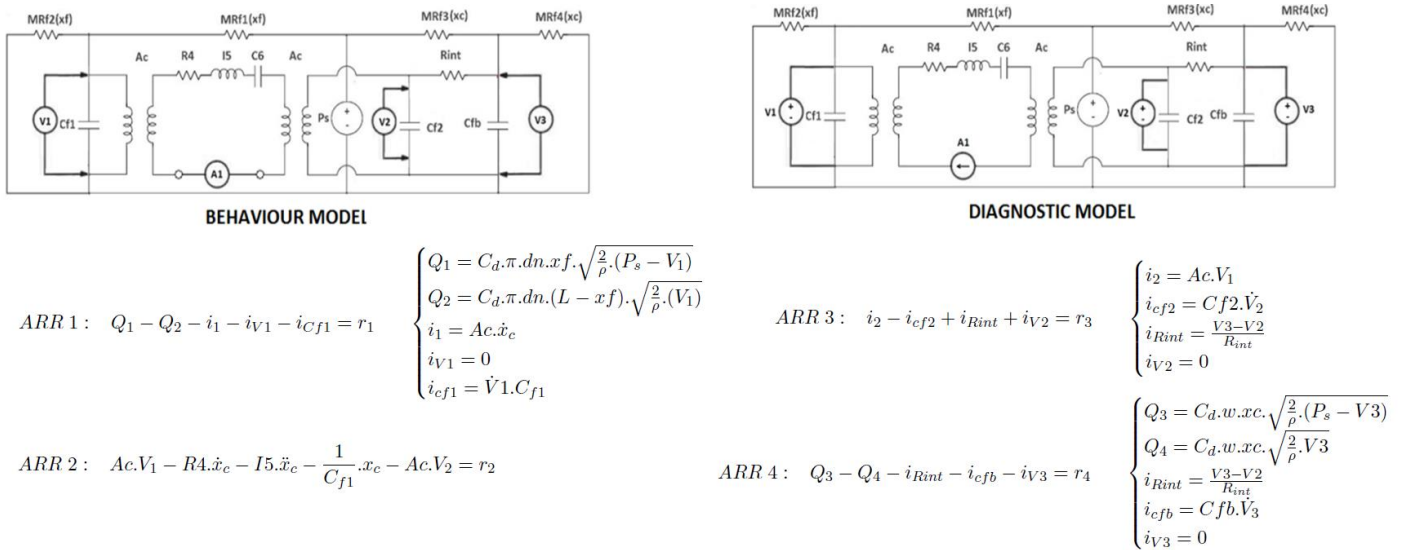


Figure 6 –Sensor placement in the behavior model, diagnostic model and ARR equations from diagnostic model.

From the ARR it is possible to obtain the fault signature matrix, shown in Table 1. The fault signature matrix makes the relationship of the residuals sensibility for each parameter in the model. Taking as an example the residual 1 (r_1), the parameters that most affect its value are Q_1 , Q_2 , Ac , and the Pc_1 measurement V_1 . So, thinking about failure modes, if there is a pressure nozzle obstruction (the nozzle that controls the flow Q_1), the flow Q_1 will be smaller and, depending on the obstruction level, the pressure Pc_1 will be significantly smaller than it would be without the nozzle obstruction, thus, the residual r_1 will not be zero anymore, if there is a pressure nozzle obstruction. The two last matrix rows relate the detectability and the isolation of the parameter fault. So, if at least in one residual row the true value

appears, then it is detectable. For example, the parameter Q1 is detectable because, if it has a disturbance from the original value, the residue 1 would be affected. For one parameter fault isolation, the pattern of the residual appearance must be unique. For example, the parameter xc (spool position) is isolable because, if there is an abnormal condition and the spool position differs from its normal movement (in a hydraulic line leakage or increased spool friction), the residuals r2 and r3 would be modified and this residual appearance pattern is unique for the xc failure mode.

Table 1 - Servo valve fault signature matrix.

	Q1	Q2	xc	Ac	Ps	V1	R4	I5	C6	V2	V3	Rint	Q3	Q4
r1	1	1	0	1	1	1	0	0	0	0	0	0	0	0
r2	0	0	1	1	0	1	1	1	1	1	0	0	0	0
r3	0	0	0	1	0	1	0	0	0	1	1	1	0	0
r4	0	0	1	0	1	0	0	0	0	1	1	1	1	1
D	1	1	1	1	1	1	1	1	1	1	1	1	1	1
I	0	0	1	0	1	0	0	0	0	1	0	0	0	0

The Figure 7 shows the simulation results (numerical evaluation of the four ARR, generating four residuals values r1, r2, r3 and r4) for different faults, applying a step input voltage in the torque motor terminals.

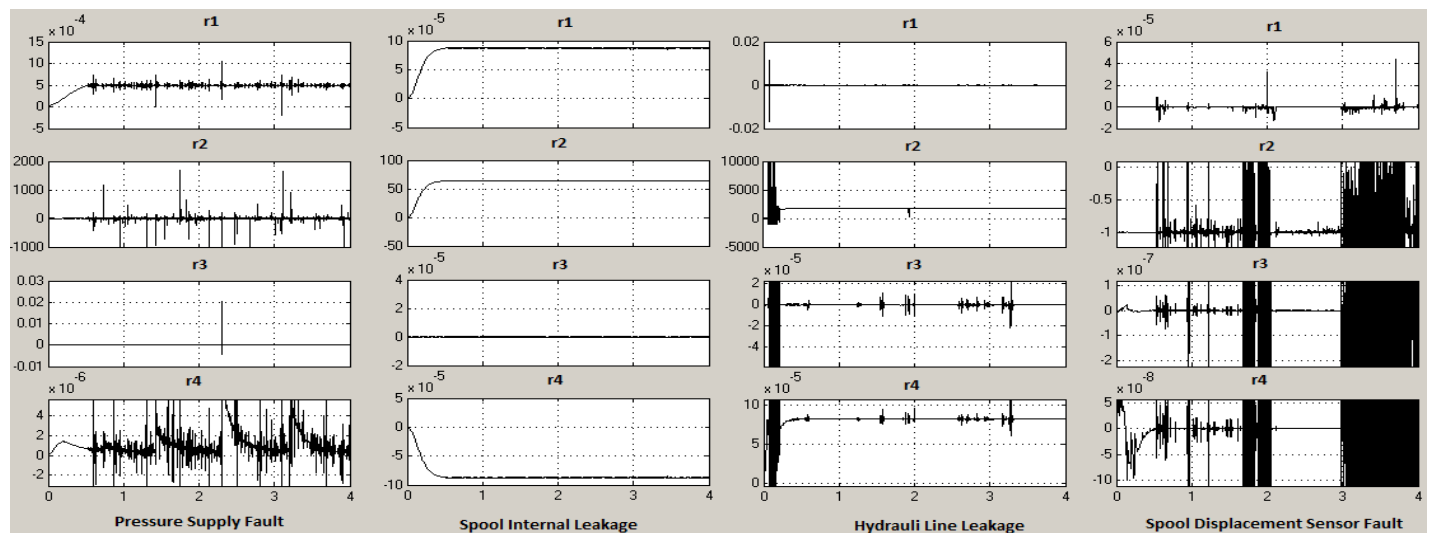


Figure 7 – Residual response for different failure modes.

With the simulations results, it is possible to see that the residual response reflects the fault signature matrix. For the pressure supply fault, the matrix indicates that the most sensitive residuals are r1 and r4. The Figure 7 indicates variation on these two residuals, as expected. Analyzing the spool internal leakage fault, the deviation occurs in more than one parameter. In this case, the most affected parameters are the spool displacement and the flows Q1, Q2 and Q3. Thus, based on the matrix, the residuals sensible to these faults are r1, r2 and r4 as confirmed by the simulation results in Figure 7. The hydraulic line leakage directly affects the spool displacement and the flows Q3 and Q4. These parameters affects the residuals r2 and r4 as confirmed by the simulation. Introducing a measure fault in the displacement sensor, caused a deviation in the residue r2, as expected according to the matrix.

CONCLUSION

The objective of this work was to develop a model for the aircraft braking dynamics and its hydraulic brake system, demonstrating, besides its normal operation behavior, what some common failure modes could cause on the system performance. The FDI method proposed was able to detect all the faults introduced. Thus, this methodology is a viable solution, helping to support early failure identification.

REFERENCES

- [1] K. Medjaher, A bond graph model-based fault detection and isolation., Brenguer and L. Jackson. Maintenance Modelling and Applications. Chapter 6 : Fault Diagnostics., Det Norske Veritas (DNV), pp.503- 512, 2011. hal-00635549
- [2] W. Borutzky, Bond Graph Model-based Fault Diagnosis of Hybrid Systems, (2016). Springer Verlag
- [3] A.K. Samantaray, K. Medjaher, B. Ould Bouamama, M. Staroswiecki, Dauphin-Tanguy Diagnostic bond graphs for online fault detection and isolation, Department of Mechanical Engineering, Indian Institute of Technology, 721 302 Kharagpur, India
- [4] Merritt, H. E., Hydraulic Control Systems, (1967). New York - London - Sydney: John Wiley and Sons